Electrodeless time-resolved microwave conductivity study of charge-carrier photogeneration in regioregular poly(3-hexylthiophene) thin films

Gerald Dicker,* Matthijs P. de Haas, Laurens D.A. Siebbeles, and John M. Warman
Department of Radiation Chemistry, IRI, Delft University of Technology, Mekelweg 15, 2629 JB Delft, The Netherlands
(Received 19 February 2004; published 13 July 2004)

The electrodeless flash-photolysis time-resolved microwave conductivity technique (FP-TRMC) has been used to study the photogeneration of charge carriers in spin-coated films of regioregular poly(3-hexylthiophene) (P3HT), over the photon energy range from 1.9 to 5.2 eV for incident light intensities from 10^{13} to 10^{16} photons/cm^2 per (3 ns) pulse. The initial, single-photon quantum yield of photoionization, ϕ, has been estimated from the low-intensity limit to the photoconductivity based on a charge carrier mobility of 0.014 cm^2/Vs (determined in separate pulse-radiolysis TRMC experiments on bulk P3HT). The value of ϕ is constant at (1.7 ± 0.4)% within the range 1.9–3.0 eV, which encompasses the first electronic absorption band of P3HT. Above 3.0 eV, ϕ increases, up to a value of (7 ± 2)% at 5.2 eV. The activation energy of the photoconductivity was found to be approximately 50 meV at all photon energies. The high-intensity, sublinear dependence of the photoconductivity can be described by the occurrence of either exciton-exciton annihilation or diffusional charge recombination with rate coefficients of 2.3×10^{-8} cm^3/s and 1.1×10^{-8} cm^3/s.

DOI: 10.1103/PhysRevB.70.045203 PACS number(s): 73.50.Pz, 73.50.Gr, 73.61.Ph, 78.70.Gq

I. INTRODUCTION

Since the synthesis of the first soluble poly(3-alkylthiophenes),[1] considerable improvements have been made in the chemical purity, molecular mass, and the regularity of the position of the solubilizing side chains.[2] It has been found that the degree of HT-HT regioregularity in the head-to-tail–head-to-tail (HT-HT) side-chain pattern (see Fig. 1) has a significant influence on the ability of individual chains to self-assemble into ordered domains at solution/substrate interfaces [3] and in solution-cast films.[4] Stacking of the planar backbones via π-electron interaction leads to the formation of lamellae, in which quasidelocalized, two-dimensional charge transport has been observed.[4–6] The field-effect charge-carrier mobility in such films is orders of magnitude higher than in films of regiorandom P3HT.[4,7,8] The high mobility (up to 0.1 cm^2/V s),[4] together with environmental stability and ease of processing, have led to the application of regioregular P3HT in "plastic electronics" prototypes.[7–9] Recently, it has been shown that the molecular weight also has a dramatic influence on the field-effect mobility.[10]

For optoelectronic applications, knowledge about the efficiency and mechanism of converting light into electricity is of crucial importance. The fundamental processes responsible for the photoconductivity in π-conjugated polymers are not fully clarified yet.[11] This originates mainly from the difficulties in interpreting the experimental photoconductivity data. Using conventional dc techniques, this is due to the following complications: (a) at the interface between the polymer and the electrode deactivation of excitons can occur.[12] (b) Charges can be injected into the polymer upon photon absorption by the electrode layers. (c) Electric fields enhance the dissociation of excitons and geminate pairs.[13] (d) The "internal filter effect" can give rise to an inverted spectral photocurrent response.[14–16] In addition, it has recently been shown that electrons photoejected from the polymer surface can make a large contribution to the measured conductivity if no precautions are taken.[17–19] Because of these potential complications, considerable uncertainty exists in the literature as to the spectral and light-intensity dependence of the intrinsic photoconductivity of conjugated polymers.

The aforementioned problems can be circumvented using the flash-photolysis time-resolved microwave conductivity technique (FP-TRMC).[20–23] This is free of electrodes and operates at low electric fields ($\leqslant$100 V/cm). Because of the high frequency of the electric field (9 GHz), charge carriers are not required to cross grain or domain boundaries, in contrast to dc conductivity measurements. As a result, the TRMC method is most sensitive to the photoconductive properties of the ordered, high-mobility domains in the film. In addition, because of the electric-field polarization of the microwaves, the in-plane anisotropy of the photoconductivity of aligned polymer layers can be measured.[24]

Charge carriers are usually detected by measuring the photoinduced conductivity or the photoinduced optical absorption whereby in the latter case the nature of the detected species has to be confirmed by spin resonance.[25] Because of the, in general, low mobilities and low quantum yields, high laser intensities are usually necessary to obtain a sufficient signal-to-noise ratio. At high laser intensities, the charge-carrier photogeneration is affected by exciton-exciton annihilation and sequential excitation.[26] At the same time, ground state bleaching and stimulated emission can occur. Additionally, charge carriers can undergo rapid bimolecular recombination.[27] These phenomena complicate the interpretation of the results such that usually only an approximate estimate of the quantum yield of charge carrier photogeneration can be given.

In this paper we report the measurement and analysis of the photon energy, laser intensity, and temperature dependence of charge-carrier photogeneration in a spin-coated layer of regioregular P3HT. From these findings, the photon

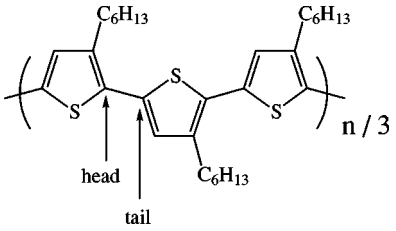

FIG. 1. Chemical structure of head-to-tail–head-to-tail coupled regioregular poly(3-*n*-hexylthiophene).

energy dependence of the low-field single-photon quantum yield of bulk charge carrier photogeneration, ϕ, has been obtained from close to the absorption onset at 1.8 eV up to 5.2 eV. The findings provide insight into the mechanism of charge-carrier photogeneration in regioregular P3HT.

II. EXPERIMENTAL

We have used two different batches of head-to-tail–head-to-tail (HT-HT) coupled regioregular poly(3-*n*-hexylthiophene) (P3HT, Fig 1), both of which showed very similar photoconductive properties. One sample was synthesized in the group of Professor R. A. J. Janssen at the Technical University of Eindhoven, The Netherlands. The degree of HT-HT regioregularity was 92% and the weight-average molecular weight, M_w, was 12.8 kg/mol with a polydispersity of 1.4, corresponding to an average of $n=55$ monomer units per chain. The other sample [$M_w=40$ kg/mol, HT-HT=96%] was a commercial sample obtained from Merck, which was donated to us by Dr. B.-H. Huisman of Philips Research Eindhoven.

Films of thickness L of 100–150 nm were prepared by spin coating a 15 g/l chloroform solution on a 12×25 mm^2, 1-mm-thick quartz substrate in air at room temperature. The thickness of the films was determined using a Veeco Dektak 8 Stylus step-Profiler. To check the influence of oxygen on the measurements, films were also prepared and handled exclusively under inert atmosphere in a nitrogen glovebox.

A Perkin-Elmer λ-900 spectrophotometer equipped with an integrating sphere was used to measure the fraction of incident light reflected and transmitted by the sample, F_R and F_T, respectively. The optical density, *OD*, defined by

$$F_T = (1 - F_R)10^{-OD}, \tag{1}$$

was derived from these measurements. The fraction of incident photons absorbed by the polymer film, F_A, is

$$F_A = I_A/I_0 = 1 - F_R - F_T. \tag{2}$$

.

The polymer-coated quartz plate was placed in a microwave resonant cavity at a position of maximum electric field strength, as illustrated in Fig. 2. The electric-field strength at the position of the sample was 100 V/cm or less and the electric-field vector was parallel to the surface of the sample. The response time of the cavity was approximately 40 ns. An additional configuration of the microwave cell was equipped

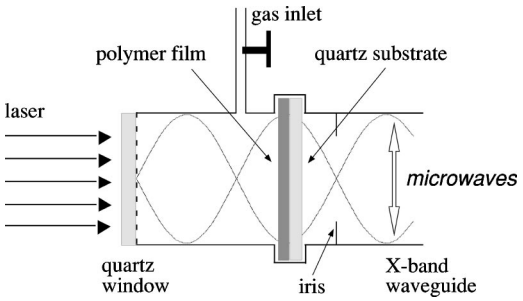

FIG. 2. Schematic representation of the microwave resonant cavity containing a thin-layer sample (not to scale). The sinusoidally varying dashed lines represent the standing-wave pattern of the microwave electric field.

with heating wires, which allowed *in situ* annealing of the film (at 373 K for 90 min in a vacuum of 10^{-4} mbar). A grating in the back wall of the cavity was covered and vacuum-sealed with a quartz window. The cavity was vacuum sealed with aramide foil at the position of the iris coupling hole and was attached to a vacuum line via a stopcock and evacuated down to a pressure of less than 10^{-4} mbar. After evacuation, the cavity was filled to atmospheric pressure with an electron scavenging gas mixture of CO_2 and SF_6 in the pressure ratio 10:1 in order to capture any highly mobile electrons that might be photoejected from the polymer surface.[17–19]

The sample was irradiated with single 3 ns full width at half maximum (FWHM) pulses from a wavelength-tunable Coherent Infinity optical parametric oscillator pumped by a Nd:YAG laser. The signal-to-noise ratio was improved by averaging up to 100 single pulses. The wavelength could be varied continuously over the ranges 700–420 nm and 310–240 nm using a second harmonic generator. The third harmonic of the pump beam at 355 nm could also be used. The pulse energy was measured using a Coherent Labmaster power meter to monitor a small fraction of the incident beam reflected by a quartz plate. The maximum pulse energy was approximately 7 mJ in the visible, and approximately 1 mJ in the UV. The intensity could be attenuated using a series of neutral density filters (Melles Griot). The cross section of the laser beam was shaped to a rectangle with dimensions closely matching the substrate size. The intensity distribution over the cross section of the beam was uniform and free of hot spots. Because of the grating, the illuminated area of the film was only 1.6 cm^2.

The photoinduced change in the conductance of the sample on flash photolysis, ΔG, was monitored as a change in the microwave power, $\Delta P/P$, reflected by the cavity at resonance (~9 GHz) using microwave circuitry and detection equipment, which has been described elsewhere.[20–23] The two parameters are related by

$$-\Delta P/P = K\Delta G, \tag{3}$$

where K is a sensitivity factor that was derived from the resonance characteristics of the cavity and the dielectric properties of the medium.

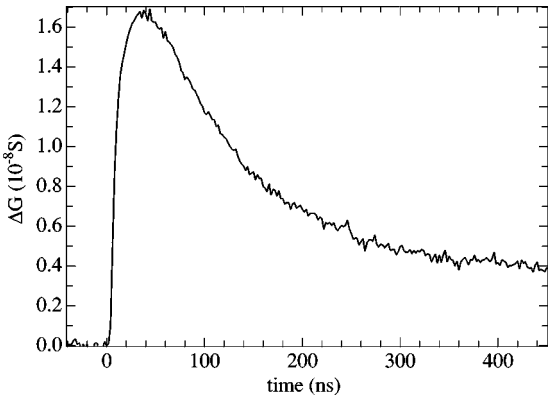

FIG. 3. The change in conductance, ΔG, of a 110-nm-thick film of P3HT on 3 ns FWHM pulsed photoexcitation at 500 nm (2.48 eV) with $I_0 = 4.3 \times 10^{15}$ photons/cm^2/pulse.

The change in conductance is related to the concentration of charge-carrier pairs, n_p, and the sum of the mobilities of the positive and the negative charge carrier, $\Sigma\mu$ $(=\mu_+ + \mu_-)$, by

$$\Delta G = \beta e \Sigma \mu \int_0^L n_p(z)\, dz, \tag{4}$$

where $n_p(z)$ is the concentration at a depth z within the photoactive layer of thickness L, e is the elementary charge, and β (=2.30) is the ratio between long and short internal dimensions of the waveguide. The microwave electric field vector is parallel to the short side.

The quantum yield of charge-carrier photogeneration, ϕ, is the fraction of primary photo-excitations that eventually lead to the formation of charge-carrier pairs,

$$\phi = \int_0^L n_p(z)\, dz / I_A, \tag{5}$$

where I_A $(=I_0 F_A)$ is the number of photons absorbed per unit area. If recombination and/or immobilization of the charge carriers is slow with respect to the pulse duration and the time resolution of detection, then the maximum conductance, reached after the laser pulse, is related to the product of the quantum yield and the mobility sum by

$$\Delta G_{\max} = \beta e F_A I_0 [\phi \Sigma \mu]. \tag{6}$$

III. RESULTS AND DISCUSSION

On pulsed photoexcitation at 2.48 eV (500 nm), i.e., close to the maximum of the first absorption band of P3HT, a readily observable transient change in the conductance of the film is observed, as shown in Fig. 3. The transient conductance reaches a maximum, $\Delta G_{\max}$, at approximately 40 ns after the start of the 3 ns FWHM laser pulse due to the relatively slow response time of the microwave cavity. The subsequent decay is nonmonoexponential and occurs over a time scale of tens to hundreds of nanoseconds. The decay time is determined by both the decrease in the conductance of the film and, in the early stages, by the response time of the cavity.

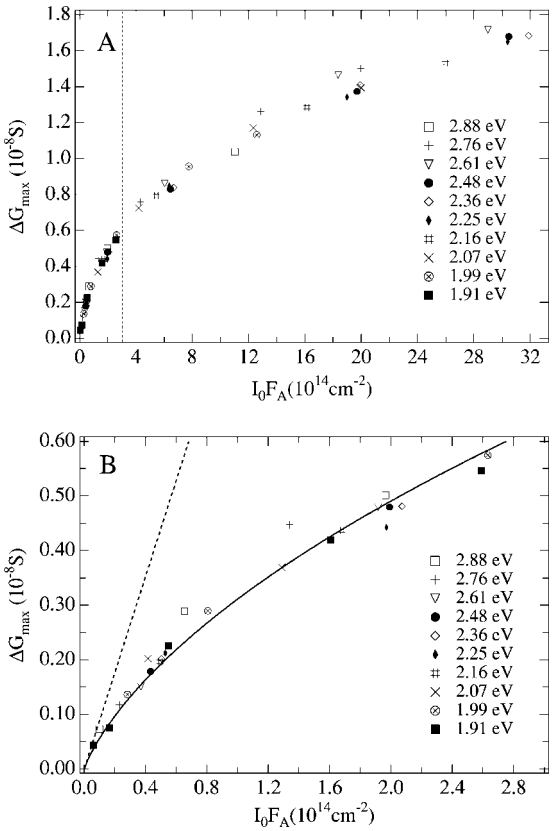

FIG. 4. (a) The dependence of the maximum photoconductance, $\Delta G_{\max}$, for a 110-nm film on the product of the incident intensity, I_0, and the fraction of photons absorbed in the sample, F_A, for photon energies below 3 eV. The data for $I_0 F_A$ values lower than indicated by the vertical dashed line are expanded in (b). (b) The full line was calculated using Eq. (7) (see text) and the dashed straight line corresponds to the limiting,low-intensity linear dependence.

The value of $\Delta G_{\max}$ increases sublinearly with laser intensity, as shown in Fig. 4(a), where $\Delta G_{\max}$ is plotted against the number of photons absorbed per unit area, $I_0 F_A$, for photon energies in the range 1.9 to 2.9 eV, i.e., encompassing the region of the first absorption band. As can be seen, the magnitude and functional dependence of $\Delta G_{\max}$ on $I_0 F_A$ is closely similar for all photon energies within this photon energy range. From this we conclude that the quantum yield for the formation of mobile charge carriers is close to constant, i.e., independent of wavelength, on excitation within the first absorption band of P3HT.

According to Eq.(6), in the absence of secondary reactions, a plot of $\Delta G_{\max}$ against $I_0 F_A$ should be a straight line of slope $\beta e[\phi \Sigma \mu]$, from which the product of the quantum yield for charge-carrier formation and the sum of the mobilities can be determined, since β and e are known constants. The sublinearity actually observed is attributed to the occurrence of secondary processes at elevated intensities, which result in a reduction of the charge-carrier pair yield below its initial value, ϕ_0. The possible secondary processes responsible for the nonlinear intensity dependence (e.g., charge re-

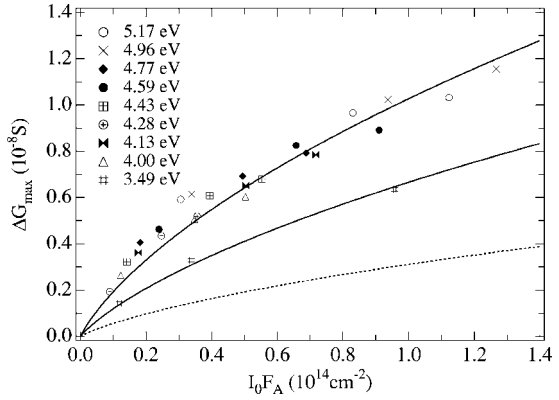

FIG. 5. The dependence of the maximum photoconductance, $\Delta G_{\max}$, for a 110-nm film on the product of the incident intensity, I_0, and the fraction of photons absorbed in the sample, F_A, for photon energies above 3 eV. All lines were calculated using Eq. (7) (see text), with the lower dotted curve the best fit to the sub 3 eV data shown in Fig. 4(b).

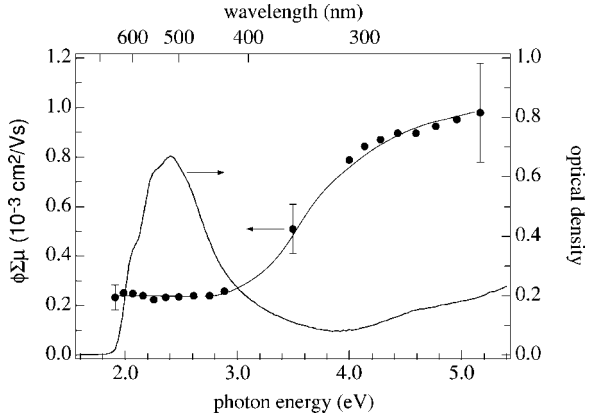

FIG. 6. The photon energy dependence of the product of the quantum yield and the mobility sum of the charge carriers, $\phi\Sigma\mu$ (points, left scale) for the spin-coated film of regioregular P3HT. The line through the data points is a guide to the eye. The optical absorption spectrum (right scale) is included for comparison.

combination, exciton-exciton annihilation, and/or product filtering) will be discussed in detail at the end of this section.

We have found that the results can be fitted quite well using an empirical expression of the form

$$\Delta G_{\max} = AI_0F_A/(1+\sqrt{BI_0F_A}). \tag{7}$$

The data follow, in other words, a linear dependence with slope A ($=\beta e[\phi\Sigma\mu]$) at the lowest intensities, changing to a square root dependence at elevated intensities. The full, curved line in Fig. 4 was calculated using Eq. (7) with $A=8.8\times10^{-23}$ S cm^2 (where S=Siemens$=1/\Omega=A/V$) and $B=3.3\times10^{-14}$ cm^2. The straight, dashed line in the figure corresponds to the limiting, low-intensity linear behavior with slope A. From the value of A, an estimate of 2.4×10^{-4} cm^2/V s can be derived for $\phi\Sigma\mu$. Since a fraction of the initially formed charge carriers may have decayed within the response time of detection, even at the lowest intensities, this value of $\phi\Sigma\mu$ represents a lower limit to the "initial" value, $\phi\Sigma\mu$.

In Fig.5 the data points are shown for photon energies in excess of 3 eV. The lowest (dotted) line in the figure corresponds to the best fit line drawn through the sub 3 eV data points in Fig. 4(b). As can be seen, the values of $\Delta G_{\max}$ for a given value of I_0F_A are significantly higher for the higher photon energies, by a factor of approximately 2 at 3.5 eV and approximately 4 above 4 eV. The sublinear nature of the $\Delta G_{\max}$ versus the I_0F_A dependence is, however, still observed at the higher photon energies and can also be reasonably well fitted with Eq. (7), as shown by the full lines in Fig. 5, which were calculated using $A=1.9\times10^{-22}$ S cm^2 and 3.2×10^{-22} S cm^2 and $B=3.3\times10^{-14}$ cm^2 and 4.6×10^{-14} cm^2 for the lower and upper full curves, respectively. The value of $\phi\Sigma\mu$ derived from the A value for the upper calculated curve is 8.7×10^{-4} cm^2/V s, i.e., a factor of 3.6 larger than the value estimated from the best fit to the sub 3 eV data. If the mobility of the charge carriers is taken to be independent of the energy of photoexcitation, then the increase by a factor of approximately 4 in A in going from the visible to the UV must reflect a substantial increase in the quantum yield of charge-carrier formation.

Relationship (7) has been used to obtain best fits for each *individual* photon energy from 1.9 to 5.2 eV. In these fits, the B parameter was found to be $(3.3\pm0.5)\times10^{-14}$ cm^2 and $(4.6\pm0.5)\times10^{-14}$ cm^2 for photon energies up to and above 3.5 eV, respectively. The low-intensity, limiting values of $\phi\Sigma\mu$ derived from the A factors are plotted as a function of photon energy in Fig. 6. The uncertainty in the absolute value of $\phi\Sigma\mu$ is ±20%, as indicated in Fig. 6.

Comparison with the optical density spectrum, also shown in Fig. 6, clearly demonstrates the constancy of the charge-carrier yield on excitation to the first, S_1, exciton level and the increase in yield on excitation to higher, S_n, levels within the singlet manifold. The constancy of the quantum yield in the 1.9–3.0 eV energy range indicates that dissociation of the S_1 exciton is not facilitated by an excess vibrational energy. This is different from the previously observed increase of the quantum yield due to dissociation of hot excitons in a ladder-type poly(para-phenylene) (MeLPPP).[28] We ascribe the lower energy plateau in Fig. 6 to the dissociation of the vibrationally relaxed S_1 exciton. The increased yield at higher photon energies can be due to autoionization[29] of the S_n states in competition with internal conversion.

We have performed experiments on samples which were prepared, annealed, and measured under an oxygen-free atmosphere. These gave the same photoconductive response as samples that were prepared under atmospheric conditions and were not annealed. This leads us to the conclusion that oxygen doping contributes negligibly to the efficiency of the photogeneration of charge carriers.

An absolute value for the quantum yield, ϕ, can be estimated if the mobility sum, $\Sigma\mu$, is known. In a *pulse-radiolysis* TRMC study,[53] we have measured the mobility of the charge carriers in a bulk sample of the same batch of P3HT as used in the present experiments and found $\Sigma\mu=0.014$ cm^2/V s. Using this value, we obtain for the quantum yield of dissociation of the S_1 exciton $\phi=0.017$. In the

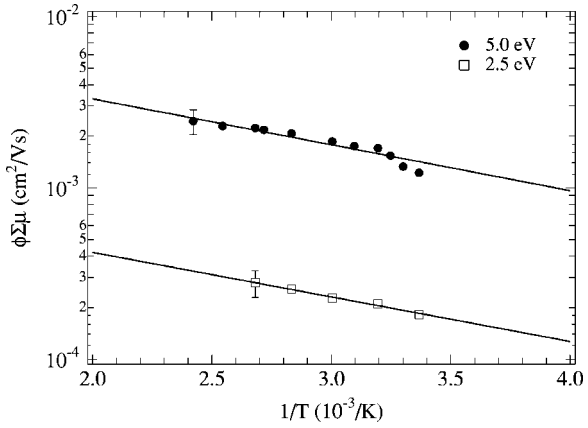

FIG. 7. Arrhenius-type plots of the product of the quantum yield and the sum of the charge-carrier mobility, $\phi\Sigma\mu$, for two different photon energies. The straight lines are fits to the data points, the slopes of which correspond to an activation energy of 52 meV and 53 meV for the 5.0 eV and the 2.5 eV data, respectively.

literature, values for the field-effect hole mobility, μ_{FE}, up to 0.1 cm^2/V s have been reported.[4,8] However, these mobility values were obtained at high dc fields whereas the pulse radiolysis value is a low field ($E<10^2$ V/cm), high-frequency value, which should be more applicable to the present FP-TRMC experiment. If, however, we take the maximum field-effect hole mobility,then we derive a lower-limit estimate of ϕ of 2.4×10^{-3}. As pointed out above, because of the limited time response of the measurements, the value of ϕ represents a lower limit to the initial yield, ϕ_0. Experiments are underway using thicker, drop-cast films, which allow the use of a faster time-response cell configuration.

The lower-limit estimate of ϕ_0 given above is still substantially higher than the quantum yield for the field-assisted dissociation of the S_1 exciton in other π-conjugated polymers reported in the literature. In dc photoconductivity measurements in which the influence of the electrode contacts on the dissociation of the excitons could be excluded by using blocking layers, the following values have been reported: for a poly(phenylenevinylene)-ether (PPV-ether) $\phi=2\times10^{-5}$ (at $E=2\times10^5$ V/cm),[12,30] for a ladder-type poly(paraphenylene) (MeLPPP) $\phi=1\times10^{-3}$ (at $E=1\times10^5$ V/cm).[13] In a time-of-flight study,[31] where no blocking layer was used, the quantum yield for regiorandom P3HT was found to be $\phi\approx2\times10^{-4}$ (at $E=1\times10^5$ V/cm).

In an attempt to shed more light on the dissociation mechanism of the excitons in regioregular P3HT, we have measured the temperature dependence of the efficiency of charge-carrier photogeneration. The values for $\phi\Sigma\mu$ at 2.5 eV are shown as open squares in the Arrhenius-type plot in Fig. 7. The straight line is a least-squares fit to the data using $X_0\exp(-E_a/k_BT)$. From the slope, the activation energy, E_a, is found to be 53 meV. In the same figure is shown, as filled circles, the data for excitation at 5.0 eV, which yields a similar activation energy, $E_a=52$ meV. The temperature dependence of $\phi\Sigma\mu$ was measured for several other photon energies between 2−5 eV, and the activation energy was found to be independent of the photon energy.

Using the pulse-radiolysis TRMC technique, we have determined the activation energy of the mobility of charge carriers in regioregular P3HT to be 28 meV. Subtracting this value from the value found for the product $\phi\Sigma\mu$ given above results in an estimate of the activation energy for charge-carrier pair formation, E_a^ϕ of 25 meV. On the basis of a simple model of the thermal dissociation of a bound exciton into free charge carriers, this value of E_a^ϕ would correspond to an S_1 exciton binding energy, E_b, of only 25−50 meV, depending on the order (first or second) of the charge-carrier decay process during the pulse. Even the upper limit, $E_b=50$ meV, seems unreasonably low.[32–36] However, a recent theoretical study on crystalline polythiophene has yielded values of E_b as low as 150 and 110 meV for the on-chain and charge-transfer exciton, respectively.[37]

We emphasize that the maximum (microwave) electric field strength in the present experiments is only approximately 100 V/cm (10^{-5} V/nm) so that field-induced exciton dissociation can be excluded. In addition, no electrode interfaces are present that could lead to charge-carrier generation via interfacial electron transfer to or from excitons. It has recently been suggested that dissociation of relaxed excitons could occur via encounter with an impurity charge-transfer center.[38] However, since the exciton diffusion length in regioregular P3HT (Ref. 39) and other polythiophene derivatives[40,41] has been estimated to be only approximately 5 nm, an unrealistically large impurity concentration would be required. This mechanism would also seem to be excluded on the basis of the close similarity of the results for the two, independently synthesized samples used.

In view of the above, we conclude that the generation of charge carriers observed on photoexcitation in the first absorption band of P3HT is an intrinsic property of the polymer itself. The relatively high value of ϕ and its low activation energy may be related to the lamellar nature of the morphology of the solid.[4,7] In a previous publication,[42] we have shown that the photoconductivity in P3HT increases by one order of magnitude in going from an 81% HT-HT spin-coated to a greater than 95% HT-HT drop-cast film. This enhancement is clearly due to the increased nanoscale ordering, which could result in a relatively high efficiency of direct optical interchain transitions, forming charge-transfer type excitons, leading to the electron and hole on separate polymer chains with, as a consequence, a higher probability of mutual escape. Evidence has recently been presented that indicates the interchain order in P3HT decreases with increasing temperature.[43] This negative effect could possibly partially counteract a thermally induced increase in the escape probability of charge-carrier pairs, thus resulting in a lower effective activation energy of ϕ.

As shown in Figs. 4 and 5, the intensity dependence of the conductance can be quite well described using the empirical equation (7), in which the paramter B is a measure of the sublinearity. For $I_0F_A=1/B$, the conductance is reduced to half of the value expected for a linear response of slope A. For the first absorption band, B is 3.3×10^{-14} cm^2, which corresponds to an average photoexcitation density of $1/BL=2.8\times10^{18}$ cm^{-3}. This is a factor of more than 1000 lower than the thiophene monomer unit concentration of $\sim4\times10^{21}$ cm^{-3} and, therefore, too low to explain the sublinear-

ity in terms of bleaching of the ground state absorption or filtering due to absorption by photoproducts, which would also be expected to be spectrally separated from the ground state absorption.[25] We, therefore, attribute the sublinearity in the intensity dependence to bimolecular interactions between neutral or charged photoexcitations.

The bimolecular interaction of the photoexcitations could be exciton-exciton annihilation. It has previously been demonstrated that exciton-exciton annihilation is indeed an important decay mechanism in P3HT at photon fluxes above $\sim 1\times 10^{14}$ cm^{-2} using subpicosecond laser pulses.[25,44] The annihilation reaction is stated as[29]

$$S_1 + S_1 \overset{\gamma_A}{\rightarrow} S_n + S_0. \tag{8}$$

If this were to lead to a higher excited state in the singlet manifold than S_1 [i.e., $n>1$ in (8)] then a superlinear dependence on light intensity would have been expected since our results indicate that the efficiency of charge separation is more than a factor of 2 larger for higher excited states (see Fig.6). However, for $n=1$ in (8) a sublinear dependence, as found, would result, and we consider the consequence of this for the form of the intensity dependence in what follows.

The exciton concentration, n_E, will reach a steady-state value during the laser pulse since the lifetime of the excitons,[45] $\tau=k^{-1}=300$ ps, is an order of magnitude shorter than the pulse length. Hence, the continuity equations stated as follows:

$$\frac{dn_E}{dt} = g - \gamma_A n_E^2 - k n_E = 0, \tag{9}$$

where $g=I_0F_A/L\Delta t$ denotes the average exciton formation rate for an idealized rectangular laser pulse of length $\Delta t = 4$ ns. The solution for the steady-state concentration is

$$n_E = \frac{2g}{k(1+\sqrt{1+4g\gamma_A/k^2})}. \tag{10}$$

The S_1 excitons may dissociate into electron-hole pairs with a probability ϕ, according to

$$S_1 \overset{\phi k}{\rightarrow} e^- + h^+. \tag{11}$$

The formation rate of the electron-hole pair concentration, n_p, is given by

$$\frac{dn_p}{dt} = \phi k n_E. \tag{12}$$

Using the conductance relation, $\Delta G=\beta L e n_p \Sigma\mu$, we get for the end-of-pulse (eop) conductance

$$\Delta G_{eop} = \frac{2e\beta\phi\Sigma\mu F_A I_0}{1+\sqrt{1+\dfrac{4\gamma_A I_0 F_A}{k^2 L\Delta t}}}. \tag{13}$$

This equation was used to fit the intensity dependence of the conductance maxima of the first absorption band; see the solid line in Fig. 8. The least-squares fit gave $\gamma_A=2.3\times 10^{-8}$ cm^3/s.

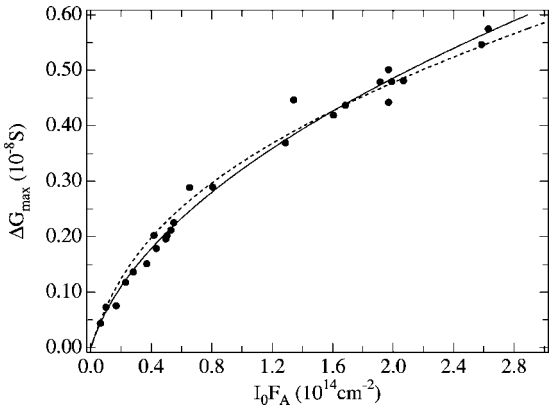

FIG. 8. The dependence of the maximum photoconductance, $\Delta G_{\max}$, on the product of the incident intensity, I_0, and the fraction of photons absorbed in the sample, F_A, for photon energies below 3 eV [data points from Fig. 4(b)]. The full and dashed lines were calculated using Eqs. (13) and (18), respectively.

The bimolecular annihilation rate constant, γ_A, can be related to the diffusion constant of the exciton, D_E, using[46]

$$\gamma_A = 4\pi R(D_E + D_E), \tag{14}$$

where R is the reaction radius. A realistic estimate for R would be in the order of 1 nm.[29] Using this value, the exciton diffusion constant, D_E, would be in the order of 10^{-2} cm^2/s. This is a very high value, being close to, or higher than, the singlet exciton diffusion coefficient typically found in high-purity organic crystals[29] and could be due to the high interchain π-orbital overlap in the lamellae. On the other hand, the value of R could be higher than the estimate of 1 nm because of the delocalized nature of the photoexcitations.[5] Furthermore, the time-independent form of γ_A might be too simplistic because it is only valid for collisonal bimolecular annihilation processes. The inclusion of a time dependence[47–49] of γ_A would, however, be beyond the scope of this work.

The bimolecular interaction of the photoexcitations could also be due to diffusional electron-hole recombination of the form

$$e^- + h^+ \overset{\gamma_R}{\rightarrow} S_0 \tag{15}$$

with the corresponding rate equation

$$\frac{dn_p}{dt} = \phi g - \gamma_R n_p^2, \tag{16}$$

whose solution is

$$n_p(t) = \sqrt{g\phi/\gamma_R}\tanh\sqrt{g\gamma_R\phi t^2}. \tag{17}$$

Using the same expression for g as above, we obtain for the end-of-pulse conductance

$$\Delta G_{eop} = e\beta\Sigma\mu\sqrt{\frac{\phi L I_0 F_A}{\Delta t\gamma_R}}\tanh\sqrt{\frac{\Delta t\gamma_R\phi I_0 F_A}{L}}. \tag{18}$$

This equation was also used to fit the intensity dependence of the conductance maxima for photoexcitation in the first ab-

sorption band, see the dashed line in Fig. 8. The least-squares fit gave $\gamma_R = 1.1 \times 10^{-8}$ cm^3/s.

In molecular liquids and homogeneous isotropic solids, the bimolecular recombination rate constant is given by the Debye equation,[50]

$$\gamma_R = \frac{e\Sigma\mu}{\epsilon_0 \epsilon_r}. \quad (19)$$

Taking $\epsilon_r = 3$ for P3HT (Ref. 54) and $\Sigma\mu = 0.014$ cm^2/V s, we calculate a value of $\gamma_R = 0.84 \times 10^{-8}$ cm^3/s, which is close to the value found experimentally.

So far, the discussion of the intensity dependence of the photoconductance has involved models that were based on the assumption of a homogeneous isotropic material. The simplicty of the models allowed an analytical treatment but did not reflect the two-dimensional layered microstructure of regioregular P3HT, which should be included in future work.

It was reported in the literature that the average width of the lamellae in a regioregular P3HT film is 95 Å.[4] The volume of a lamella of this width would be 3.4×10^{-19} cm^3 for the present P3HT sample. This is calculated based upon a polymer chain length of 55 thiophene units with a repeat unit length of 3.9 Å and an interlamellar distance of 16.7 Å.[51] Interestingly, this volume is close to the critical volume per photexcitation, *BL*, of 3.6×10^{-19} cm^3 at which bimolecular interactions begin to dominate the decay process in the present work. We therefore conclude that if more than one photoexcitation is formed within a lamella, this leads to rapid bimolecular intralameller recombination of the photoexcitations.

IV. CONCLUSION

The photoconductivity in spin-coated films of regioregular P3HT was measured using the FP-TRMC technique. The photogeneration of charge carriers was investigated as a function of photon energy, temperature, and laser intensity.

The product of the intrinsic quantum yield of charge-carrier formation, ϕ, and the sum of the mobility of the electron and the hole, $\Sigma\mu$, was determined from close to the absorption onset at 1.9 eV up to 5.2 eV. Using $\Sigma\mu = 0.014$ cm^2/V s, obtained from a pulse-radiolysis TRMC measurement on the same materials, we find that ϕ has a constant value of 0.017 in the range of the first π-π^* absorption band, between 1.9–3.0 eV. We conclude that the formation of charge carriers is due to the dissociation of the vibrationally relaxed S_1 exciton. We attribute the high dissociation yield to the lamellar microstructure of the polymer. For photon energies in excess of 3.0 eV, ϕ increases, reaching a value of 0.07 at 5.2 eV. We attribute the increased yield at higher photon energies to autoionization of the S_n states in competition with internal conversion.

At elevated laser-pulse intensities producing more than 10^{18} photoexcitations per cubiccentimeter, the yield of charge carriers is reduced due to either exciton-exciton annihilation with an annihilation rate constant of $\gamma_A = 2.3 \times 10^{-8}$ cm^3/s or bimolecular charge-carrier recombination with a recombination rate constant of $\gamma_R = 1.1 \times 10^{-8}$ cm^3/s.

From the temperature dependence of the photoconductivity, an activation energy of 53 meV is determined. Taking into account an activation energy of 28 meV for the charge-carrier mobility results in a net activation energy for the quantum yield of charge-carrier formation of 25 meV. This surprisingly low activation energy for exciton dissociation could possibly be due to a negative compensating effect on charge separation of decreasing interchain structural order with increasing temperature, as found recently.[43]

We conclude that the nanomorphology in undoped π-conjugated polymers is vital for the efficient intrinsic photogeneration of long-lived charge carriers. We propose that control over the nanomorphology is the key to developing highly efficient light-to-electricity converting devices based on a single material.

ACKNOWLEDGMENTS

We gratefully acknowledge Professor. R. A. J. Janssen of the Technical University of Eindhoven for providing one of the polymer samples. This work is part of the research program of the Stichting voor Fundamenteel Onderzoek der Materie (FOM, financially supported by NWO) and Philips Research.

*Electronic address: g.dicker@iri.tudelft.nl

[1] K. Y. Jen, R. Oboodi, and R. L. Elsenbaumer, Polym. Mater. Sci. Eng. **53**, 79 (1985).

[2] R. D. McCullough, in *Handbook of Oligo- and Polythiophenes* edited by D. Fichou (Wiley-VCH, Weinheim, 1999).

[3] E. Mena-Osteritz, A. Meyer, B M.W. Langeveld-Voss, R. A. J. Janssen, E. W. Meijer, and P. Bäuerle, Angew. Chem., Int. Ed. **39**, 2680 (2000).

[4] H. Sirringhaus, P. J. Brown, R. H. Friend, M. M. Nielssen, K. Bechgaard, B. M. W. Langeveld-Voss, A. J. H. Spiering, R. A. J. Janssen, E. W. Meijer, P. Herwig, and D. M. de Leeuw, Nature (London) **401**, 685 (1999).

[5] R. Österbacka, C. P. An, X. M. Jiang, and Z. V. Vardeny, Science **287**, 839 (2000).

[6] P. J. Brown, H. Sirringhaus, M. Harrison, M. Shkunov, and R. H. Friend, Phys. Rev. B **63**, 125204 (2001).

[7] Z. Bao, A. Dodapalapur, and A. Lovinger, Appl. Phys. Lett. **69**, 4108 (1996).

[8] H. Sirringhaus, N. Tessler, and R. H. Friend, Science **280**, 1741 (1998).

[9] N. Stutzmann, R. H. Friend, and H. Sirringhaus, Science **299**, 1881 (2003).

[10] R. J. Kline, M. D. McGehee, E. N. Kadnikova, J. Liu, and J. M.J. Fréchet, Adv. Mater. (Weinheim, Ger.) **15**, 1519 (2003).

[11] *Primary Photoexcitations* in *Conjugated Polymers: Molecular Exciton versus Semiconductor Band Model*, edited by N. Saric-

iftci (World Scientific, Singapore, 1997).
[12] S. Barth and H. Bässler, Phys. Rev. Lett. **79**, 4445 (1997).
[13] D. Hertel, E. Soh, H. Bässler, and L. Rothberg, Chem. Phys. Lett. **361**, 99 (2002).
[14] N. T. Binh, M. Gailberger, and H. Bässler, Synth. Met. **47**, 77 (1992).
[15] A. Köhler, D. A. dos Santos, D. Beljonne, Z. Shuai, J.-L. Brédas, A. B. Holmes, A. Kraus, K. Müllen, and R. H. Friend, Nature (London) **392**, 903 (1998).
[16] S. B. Lee, K. Yoshino, J. Y. Park, and Y. W. Park, Phys. Rev. B **61**, 2151 (2000).
[17] B. R. Wegewijs, G. Dicker, J. Piris, A. Alba García, M. P. de Haas, and J. M. Warman, Chem. Phys. Lett. **332**, 79 (2000).
[18] D. Moses, C. Soci, P. Miranda, and A. Heeger, Chem. Phys. Lett. **350**, 531 (2001).
[19] G. Dicker, M. P. de Haas, and J. M. Warman, in *Proceedings of the International School of Physics "Enrico Fermi" Course CXLIX* edited by V. M. Agranovich and G. C. L. Rocca (IOS Press, Amsterdam, 2002).
[20] M. P. de Haas and J. M. Warman, Chem. Phys. **73**, 35 (1982).
[21] J. M. Warman and M. P. de Haas, in *Pulse Radiolysis*, edited by Y. Tabata (Chemical Rubber, Boca Raton, Fl, 1991).
[22] T. J. Savenije, M. P. de Haas, and J. M. Warman, Z. Phys. Chem. (Munich) **212**, 201 (1999).
[23] T. J. Savenije, M. J.W. Vermeulen, M. P. de Haas, and J. M. Warman, Sol. Energy Mater. Sol. Cells **61**, 9 (2000).
[24] F. C. Grozema, T. J. Savenije, M. J. W. Vermeulen, L. D. A. Siebbeles, J. M. Warman, A. Meisel, D. Neher, H.-G. Nothofer, and U. Scherf, Adv. Mater. (Weinheim, Ger.) **13**, 1627 (2001).
[25] O. J. Korovyanko, R. Österbacka, X. M. Jiang, Z. V. Vardeny, and R. A. J. Janssen, Phys. Rev. B **64**, 235122 (2001).
[26] M. A. Stevens, C. Silva, D. M. Russell, and R. H. Friend, Phys. Rev. B **63**, 165213 (2001).
[27] M. Westerling, C. Vijila, R. Österbacka, and H. Stubb, Chem. Phys. **286**, 315 (2003).
[28] V. I. Arkhipov, E. V. Emelianova, and H. Bässler, Phys. Rev. Lett. **82**, 1321 (1999).
[29] M. Pope and C. E. Swenberg, *Electronic Processes in Organic Crystals and Polymers* (Oxford University Press, Oxford, 1999).
[30] S. Barth, H. Bässler, H. Rost, and H. H. Hörhold, Phys. Rev. B **56**, 3844 (1997).
[31] R. Österbacka, K. Genevičius, A. Pivrikas, G. Juška, K. Arlauskas, T. Kreouzis, D. D.C. Bradley, and H. Stubb, Synth. Met. **139**, 811 (2003).
[32] M. Liess, S. Jeglinski, Z. V. Vardeny, M. Ozaki, K. Yoshino, Y. Ding, and T. Barton, Phys. Rev. B **56**, 15712 (1997).
[33] K. Sakurai, H. Tachibana, N. Shiga, C. Terakura, and M. Matsumoto, Phys. Rev. B **56**, 9552 (1997).
[34] J.-W. van der Horst, P. A. Bobbert, M. A. J. Michels, G. Brocks, and P. J. Kelly, Synth. Met. **101**, 333 (1999).
[35] J.-W. van der Horst, P. A. Bobbert, M. A. J. Michels, G. Brocks, and P. J. Kelly, Phys. Rev. Lett. **83**, 4413 (1999).
[36] J.-W. van der Horst, P. A. Bobbert, P. H. L. de Jong, M. A.J. Michels, G. Brocks, and P. J. Kelly, Phys. Rev. B **61**, 15817 (2000).
[37] J.-W. van der Horst, P. A. Bobbert, and M. A. J. Michels, Phys. Rev. B **66**, 035206 (2002).
[38] V. I. Arkhipov, E. V. Emelianova, and H. Bässler, Chem. Phys. Lett. **383**, 166 (2004).
[39] J. E. Kroeze, T. J. Savenije, M. J.W. Vermeulen, and J. M. Warman, J. Phys. Chem. B **107**, 7696 (2003).
[40] L. A. A. Petterson, L. S. Roman, and O. Inganäs, J. Appl. Phys. **86**, 487 (1999).
[41] M. Theander, A. Yartsev, D. Zigmantas, V. Sundström, W. Mammo, M. R. Andersson, and O. Inganäs, Phys. Rev. B **61**, 12957 (2000).
[42] G. Dicker, T. J. Savenije, B. H. Huisman, D. M. de Leeuw, M. P. de Haas, and J. M. Warman, Synth. Met. **137**, 863 (2003).
[43] P. J. Brown, D. S. Thomas, A. Köhler, J. S. Wilson, J.-S. Kim, C. M. Ramsdale, H. Sirringhaus, and R. H. Friend, Phys. Rev. B **67**, 064203 (2003).
[44] E. S. Maniloff, V. I. Klimov, and D. W. McBranch, Phys. Rev. B **56**, 1876 (1997).
[45] L. Magnani, G. Rumbles, I. D. W. Samuel, K. Murray, S. C. Moratti, A. B. Holmes, and R. H. Friend, Synth. Met. **84**, 899 (1997).
[46] P. W. Atkins, *Physical Chemistry* (Oxford University Press, Oxford, 1994).
[47] D. Vacar, E. S. Maniloff, D. W. McBranch, and A. J. Heeger, Phys. Rev. B **56**, 4573 (1997).
[48] A. Dogariu, D. Vacar, and A. J. Heeger, Phys. Rev. B **58**, 10218 (1998).
[49] C. Daniel, L. M. Herz, C. Silva, F. J. M. Hoeben, P. Jonkheijm, A. P. H. J. Schenning, and E. W. Meijer, Phys. Rev. B **68**, 235212 (2003).
[50] P. Debye, Trans. Electrochem. Soc. **82**, 265 (1942).
[51] T. Kawai, M. Nakazono, R. Sugimoto, and K. Yoshino, J. Phys. Soc. Jpn. **61**, 3400 (1992).
[52] H. Bässler, in *Semiconducting Polymers*, edited by G. Hadziioannou and P. F. van Hutten (Wiley-VCH, Weinheim, 1999).
[53] G. Dicker , M. P. de Haas, J. M. Warman, D. M. de Leeuw, and L D. A. Siebbeles, Phys. Rev. B (to be published).
[54] A typical value for pristine conjugated polymers, see Ref. 52.